Available online at **www.joac.info**

ISSN: 2278-1862

Journal of Applicable Chemistry

2018, 7 (6): 1636-1643

(International Peer Reviewed Journal)

Synthesis and Characterization of Mn_3O_4 Nanoparticle: A Catalyst for Synthesis of Tetrahydro-1H-pyrano[2,3-d]pyrimidine Derivatives

S. Shabir Bhat[1], Piyush Masih[1*], M. A.Shah[2], Tariq Ahmad War[3], Khursheed Ansari[4], Rajeev Lohiya[4] and Toyaj Shukla[4]

1. Department of Physics, Sam higginbottom University of Agriculture, Technology and Sciences, Allahabad (U.P)-211007, **INDIA**
2. P.G Department of Physics, National Institute of Technology, Srinagar, **INDIA**
3. Department of Physics, S.P College, Srinagar, **INDIA**
4. Department of Chemistry, University of Allahabad (U.P)-211005, **INDIA**

Email: shahidphy0@gmail.com

Accepted on 12th October, 2018

ABSTRACT

A mild and low temperature route has been developed for the synthesis of Mn_3O_4 nanoparticles by mixing aqueous solution of $Mn(CH_3CO_2)_2$ and KOH as an oxidizing agent in a simple hydrothermal reaction system in the absence of any templates, catalysts, or organic reagents. The synthesized nanoparticle of metal oxide were characterized by means of X-ray diffraction, UV-Visible spectrometry, Scanning electron microscope (SEM) and Transmission electron microscope (TEM). The crystal size of the synthesized metal chemical compound nanoparticle was obtained from X-ray diffraction study and it was found to 50± 5nm Mn_3O_4 nanocrystaline. The synthesized catalyst (Mn_3O_4) were used for activation of organic reagents lead to biologically potent tetrahydro-1H-pyrano[2,3-d] pyrimidine derivatives. The current methodologies both for the synthesis of nanocatalyst and then its application for heterocyclic synthesis disclose unique way of novel research.

Graphical Abstract

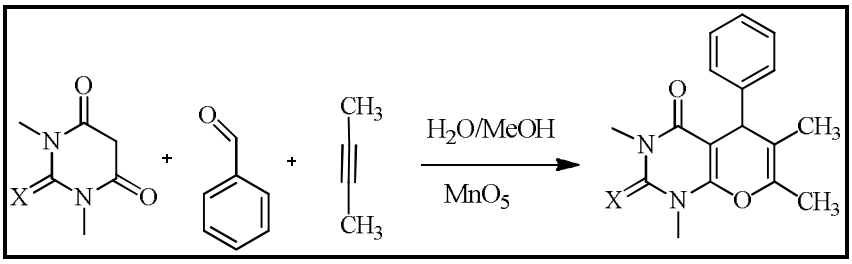

Synthetic scheme of designing *tetrahydro-1H-pyrano[2,3-d] pyrimidine derivatives*

Keywords: Mn_3O_4, Nanoparticle, Hydrothermal synthesis, XRD, SEM, TEM, Crystal growth, Tetrahydro-1H-pyrano[2,3-d]pyrimidine.

INTRODUCTION

Manganese oxides of various oxidation states and different structures have been attracting considerable research interest due to their promising application potentials in several fields, such as catalysis, magnetic materials, molecular adsorption and energy storage [1-3]. Among these manganese oxides, Mn_3O_4 is known to be an active catalyst in several oxidations and reductions, and can be used as an effective and inexpensive one to limit the emission of NOx and CO from waste gas [4, 5]. Moreover, Mn_3O_4 has was used as one of the raw materials to produce soft magnetic materials, such as manganese zinc ferrite [6]. Recent reports have indicated that Mn_3O_4 has the potential application as electrode materials for lithium ion batteries [7–8] and supercapacitors [9–13]. Mn_3O_4 synthesis has gained significant attention due to its wide range of applications, such as high-density magnetic storage media, catalysts for the decomposition of exhaust gas NOx, oxidation of methane and carbon monoxide, ion exchange, molecular adsorption, electrochemical materials, solar energy transformation, selective reduction of nitrobenzene. It has been shown to be a corrosion-inhibiting pigment for epoxypolyamide and epoxy-ester based paints. It is also a starting material in manufacturing soft magnetic materials such as manganese zinc ferrite, used in power supply transformer cores [14–25]. The conventional high temperature calcination preparation of Mn_3O_4 leads to inconsistency in product quality and is uneconomic. The sol-gel method has had been found to be expensive, time consuming and polluting. Recently, Mn_3O_4 has been prepared by microwave irradiation [26]. In recent years, different precipitation approaches based on hydrothermal or solvothermal methods have been reported [27-29]. This allows synthesis at a far lower temperature than calcination but it requires a long reaction time (48 to 72 h) at elevated temperature and pressures. All these methods form Mn_3O_4 only at temperatures well above 100°C. However, the gel to crystalline conversion method forms final products around 100°C. Earlier studies showed the structural changes and modifications of ratio of Mn and O among the different oxidation states of Mn strongly affected the properties like transportation [30-32] and magnetism [33]. Moreover, the same materials with different morphologies and structures as reported suggested that the key factor to control the properties of oxides of Mn is preparation technique. Consequently, it is indispensable to synthesize size and shape controlled Mn_3O_4 NPs viaa gel formation route at low temperature and study of their thermal stability and phase transformation with crystal structure and surface morphology upon heat treatment temperature. In the present study, attempt has been made to synthesize Mn_3O_4NPs through an aqueous gel formation route using KOH as an oxidizing agent and glycerol as a reducing agent as it is easily available, non-toxic, non-hazardous, non-volatile and recyclable liquid. The report will focus on the temperature dependent phase transformation and stability of the crystalline states in a temperature range from 80°C to 300°C to explore the different oxides of Mn and their surface morphologies.

The second part of our research plan was the application of synthesized nanocatalyst in different fields. Herein we applied Mn_3O_4 for the synthesis of tetrahydro-1H-pyrano[2,3-d]pyrimidine derivatives from thiobarbuteric acid, aldehydes and acetylene using combination of water: ethanol as a solvent at 60°C. Tetrahydro-1H-pyrano[2,3-d]pyrimidine is one of the privileged molecules with strong anticancer activity. Derivatives of benzofuran also show antibacterial, antifungal, antiviral, antitumor and antdiabetic etc. Therefore, in this study five derivatives of Benzofuran were synthesized (Scheme 1).

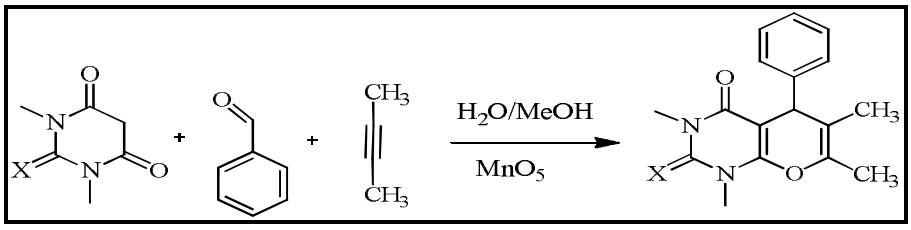

Scheme 1. Synthetic scheme of designing tetrahydro-1H-pyrano[2,3-d]pyrimidine derivatives.

MATERIALS AND METHODS

Materials: Reagent-grade KOH was purchased from Sigma-Aldrich, $Mn(CH_3CO_2)_2$ (>99.0%) was purchased from the Shanghai Chemical chemical agent Co. All solutions for the experiment were ready with double distilled (DD) water.

Material Preparation: All chemicals utilized in this study were of analytical grade and used while not more purification. During a typical procedure, the nanomaterial's were synthesized by hydrothermal method. The metal oxide manganese oxide nanoparticles was synthesized by taking 0.1 M of KOH, $Mn(CH_3CO_2)_2$ (2 mmol) and KOH (10 mmol) were severally dissolved in water (100 mL) and stirred within the sonication bathtub for 30 min. after, the KOH was introduced into above aqueous solution under stirring and the mixture was incessantly stirred for 3h at 80 ^{0}C temperature, the resulting in a brown aqueous solution and which were then transferred into Teflon lined stainless steel autoclaves, sealed and maintained at 200°C for 12 h. After the reaction completed, the resulted brown solid products were centrifugalized, washed with deionized water and ethanol to remove the ions possibly remaining in the final product, and finally dried at 60°C in air. The Mn_3O_4 synthesized was loaded in a quartz boat and put into the hot zone of a tube furnace. The temperature of the furnace was raised to 300°C and maintained at this temperature for 3 h. The obtained brown powder was collected for characterization.

The obtained samples were characterized for their structural, optical and surface morphological properties. X-ray diffraction pattern (XRD) were recorded using X-ray diffractometer (X' pert PAN Analytical) with Cu Kα radiation (λ=1.5405Å). Morphological studies were carried out using scanning microscope (JEOL SEI 25.0 kv), the transmission electron microscopy (TEM) studies were carried out usinga JEOL electron microscope operating at an accelerating voltage of 200 kv. Optical properties were studied using UV-Vis Spectrophotometer.

General Information: The reactions were performed in an open borosil round bottom flask, Analytical thin layer chromatography (TLC) was performed on precoated silica gel 60 F254 plates and visualization on TLC was achieved by UV light (254 and 354 nm). Melting points are uncorrected and were determined on a Buchi Melting point apparatus.The ^{1}H NMR spectra were recorded on a Gemini 400 MHz FT NMR spectrometer; the chemical shifts were reported on δ ppm relative to TMS. The mass spectra were recorded on Shimadzu LCMS-QP8000, LC-MS and AB-4000 Q-trap LC-MS/MS. Elemental analysis for C, H, and N were performed on Perkin Elmer model 2400 CHNS/O analyzer at SAIF Chandigarh.

Procedure for synthesis of tetrahydro-1H-pyrano[2,3-d]pyrimidine: A mixture of Benzaldehyde **1** (2.0 mmol), 2-Thiobarbeturic acid **2** (2.0 mmol), DMAD **3** (2.0 mmol) in water:methanol 1:1 ratio (10 mL), nano catalyst MnO_5 (0.5 mmol), was stirred under reflux upto 5 h. After completion of the reaction as indicated by TLC, 25mL ethyl acetate was added to the reaction mixture and stirred well. The reaction mixture was worked out and dried to slurry for column chromatography. The column was run upto 8% of ethyl acetate hexane mixture to afford pure product **4** (74-94%).

Spectral Data

Diethyl 2,3,4,5-tetrahydro-4-oxo-5-phenyl-2-thioxo-1*H*-pyrano[2,3-*d*]pyrimidine-6,7-dicarboxylate (4a): ^{1}HNMR (400 MHz, DMSO): δ 13.50 (s, 1H, NH), 12.00 (s, 1H, NH), 7.12-6.86 (m, 5H, H-Ar), 5.29 (q, 2H, CH_2), 4.46 (q, 2H, CH_2), 3.99 (s, 1H, CH), 1.24 (t, 3H, CH_3), 1.20 (t, 3H, CH_3); ^{13}CNMR (100 MHz, DMSO): δ 174.7, 173.9, 169.5, 165.5, 164.9, 155.3, 142.6, 129.6, 128.3, 125.7, 115.1, 84.3, 63.7, 41.5, 16.1; EIMS: (*m/z*): 402 (M^+). Anal. calcd for: $C_{19}H_{18}N_2O_6S$: C, 56.71; H, 4.51; N, 6.96; found C, 56.70; H, 4.45; N, 6.93.

Diethyl 2,3,4,5-tetrahydro-5-(3-nitrophenyl)-4-oxo-2-thioxo-1*H*-pyrano[2,3-*d*]pyrimidine-6, 7-dicarboxylate (4b): ^{1}HNMR (400 MHz, DMSO): δ 13.1 (s, 1H, NH), 11.02 (s, 1H, NH), 8.16 (s, 1H, H-Ar), 8.05-7.83 (m, 3H, H-Ar), 5.49 (q, 2H, CH_2), 4.59 (q, 2H, CH_2), 3.84 (s, 1H, CH), 1.23 (t, 3H,

CH_3), 1.27 (t, 3H, CH_2); ^{13}CNMR (100 MHz, DMSO): δ 185.2, 180.3, 175.0, 16.8, 161.3, 155.2, 157.9, 144.2, 131.1, 132.6, 125.9, 101.8, 85.0, 49.0, 67.5, 17.3; EIMS: (*m/z*): 447 (M^+). Anal. calcd for $C_{20}H_{19}N_3O_8$: C, 52.06; H, 4.15; N, 9.11; found C, 52.04; H, 4.12; N, 9.11.

Diethyl 5-(4-bromophenyl) -2,3,4,5-tetrahydro-4-oxo-2-thioxo-1*H*-pyrano[2,3-*d*] pyrimidine-6,7-dicarboxylate (4c): ^{1}HNMR (400 MHz, DMSO): δ 13.12 (s, 1H, NH), 11.25 (s, 1H, NH), 7.10-7.87 (m, 4H, H-Ar), 5.24 (q, 2H, CH_2), 4.44 (q, 2H, CH_2), 3.84 (s, 1H, CH), 1.28 (t, 3H, CH_3), 1.21 (t, 3H, CH_3); ^{13}CNMR (100 MHz, DMSO): δ 176.1, 172.3, 166.3, 165.8, 160.5, 154.3, 146.4, 131.1, 129.2, 120.5, 111.8, 83.5, 63.7, 40.4, 16.3; EIMS: (*m/z*): 480 (M^+). Anal. calcd for: $C_{19}H_{17}BrN_2O_6S$: C, 47.41; H, 3.56; N, 5.82; found C, 47.40; H, 3.53; N, 5.80.

Diethyl 5-(4-chlorophenyl) -2,3,4,5-tetrahydro-4-oxo-2-thioxo-1*H*-pyrano[2,3-*d*] pyrimidine-6,7-dicarboxylate (4d): ^{1}HNMR (400 MHz, DMSO): δ 12.94 (s, 1H, NH), 11.65 (s, 1H, NH), 7.12-7.37 (m, 4H, H-Ar), 5.20 (q, 2H, CH_2), 4.26 (q, 2H, CH_2), 3.96 (s, 1H, CH), 1.24 (t, 3H, CH_3), 1.21 (t, 3H, CH_3); ^{13}CNMR (100 MHz, DMSO): δ 178.1, 174.3, 168.3, 164.8, 161.5, 156.3, 145.3, 133.4, 132.9, 129.4, 118.8, 83.0, 64.4, 42.7, 15.2; EIMS: (*m/z*): 436 (M^+). Anal. calcd for: $C_{19}H_{17}ClN_2O_6S$: C, 52.24; H, 3.92; Cl, 8.12; N, 6.41; found C, 52.20; H, 3.45; Cl, 8.05; N, 6.21.

Diethyl 2,3,4,5-tetrahydro-5-(4-hydroxyphenyl)-4-oxo-2-thioxo-1*H*-pyrano[2,3-*d*]pyrimidine-6,7 - dicarboxylate (4e): ^{1}HNMR (400 MHz, DMSO): δ 13.45 (s, 1H, NH), 11.23 (s, 1H, NH), 7.25-6.81 (m, 4H, H-Ar), 5.25 (brs, 1H, OH), 5.04 (q, 2H, CH_2), 4.45 (q, 2H, CH_2), 3.34 (s, 1H, CH), 1.23 (t, 3H, CH_3), 1.21 (t, 3H, CH_3); ^{13}CNMR (100 MHz, DMSO): δ 179.3, 173.4, 166.3, 165.5, 163.2, 157.5, 156.7, 151.5, 138.1, 131.6, 114.2, 86.01, 69.3, 41.2, 16.1; EIMS: (*m/z*): 418 (M^+). Anal. calcd for: $C_{19}H_{18}N_2O_7S$: C, 54.54; H, 4.34; N, 6.70; found C, 54.50; H, 4.25; N, 6.45.

Diethyl 2,3,4,5-tetrahydro-5-(3-hydroxyphenyl)-4-oxo-2-thioxo-1*H*-pyrano[2,3-*d*]pyrimidine-6,7 - dicarboxylate (4f): ^{1}HNMR (400 MHz, DMSO): δ 13.21 (s, 1H, NH), 11.44 (s, 1H, NH), 7.32 (s, 1H, H-Ar), 7.01-6.79 (m, 4H, H-Ar), 5.35 (brs, 1H, OH), 5. 21 (q, 2H, CH_2), 4.35 (q, 2H, CH_2), 3.38 (s, 1H, CH), 1.26 (t, 3H, CH_3), 1.23 (t, 3H, CH_3); ^{13}CNMR (100 MHz, DMSO): δ 174.3, 174.6, 167.2, 165.9, 165.8, 157.7, 154.7, 140.5, 134.6, 124.3, 115.7, 113.7, 111.9, 87.6, 63.3, 41.1, 15.6; EIMS: (*m/z*): 418 (M^+). Anal. calcd for: $C_{19}H_{18}N_2O_7S$: C, 54.54; H, 4.34; N, 6.70; found C, 54.52; H, 4.25; N, 6.41.

Diethyl 2,3,4,5-tetrahydro-5-(3,4-dimethoxyphenyl)-4-oxo-2-thioxo-1*H*-pyrano[2,3-*d*]pyrimidine - 6,7-dicarboxylate (4g): ^{1}HNMR (400 MHz, DMSO): δ 13.05 (s, 1H, NH), 12.01 (s, 1H, NH), 7.20 (s, 1H, H-Ar), 7.05 (d, 1H, H-Ar), 6.93 (d, 1H, H-Ar), 5.03 (q, 2H, CH_2), 4.44 (q, 2H, CH_2), 3.93 (s, 6H, CH_3), 3.35 (s, 1H, CH), 1.24 (t, 3H, CH_3), 1.22 (t, 3H, CH_3); ^{13}CNMR (100 MHz, DMSO): δ 176.1, 173.9, 163.7, 169.9, 168.4, 159.7, 155.6, 146.5, 135.2, 122.6, 115.1, 113.6, 112.3, 84.5, 65.7, 56.3, 43.1, 15.3; EIMS: (*m/z*): 462 (M^+). Anal. calcd for: $C_{21}H_{22}N_2O_8S$: C, 54.54; H, 4.79; N, 6.06; found C, 54.56; H, 4.73; N, 6.02.

Diethyl 2,3,4,5-tetrahydro-5-(4-methoxyphenyl)-4-oxo-2-thioxo-1*H*-pyrano[2,3-*d*]pyrimidine-6,7 -dicarboxylate (4h): ^{1}HNMR (400 MHz, DMSO): δ 13.56 (s, 1H, NH), 12.04 (s, 1H, NH), 7.12-6.86 (m, 4H, H-Ar), 5.23 (q, 2H, CH_2), 4.22 (q, 2H, CH_2), 3.96 (s, 1H, CH), 3.76 (s, 3H, CH_3), 1.28 (t, 3H, CH_3), 1.24 (t, 3H, CH_3); ^{13}CNMR (100MHz,DMSO): δ 176.5, 173.2, 169.1, 165.2, 164.0, 155.7, 153.4, 139.6,134.7, 114.9, 114.3, 84.2, 65.5, 55.2, 42.1, 15.9; EIMS: (*m/z*): 432 (M^+). Anal. calcd for: $C_{20}H_{20}N_2O_7S$: C, 55.55; H, 4.66; N, 6.48; found C, 54.56; H, 4.65; N, 6.49.

RESULTS AND DISCUSSION

X-Ray Diffraction Studies: The XRD patterns of the obtained products are shown in figure 1. All of the XRD peaks in the figure 1 can be readily indexed to aorthorhombic phase of Mn_3O_4. No characteristic peaks of impurity phases are present in the fig. 1 indicating the high purity of the final

products. Moreover, the Mn_3O_4 prepared by the hydrothermal process. From the XRD peak, the Mn_3O_4 average crystal size of particles was calculated from Debye Scherer formula D= 0.9λ/ (β cosθ) wherever λ is that the wavelength of X-rays used (1.5405Å), β is the Full Width Half Maximum (FWHM) in radianand θ is theangle of diffraction.

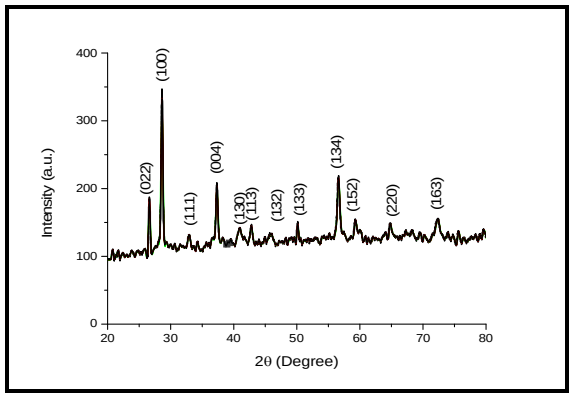

Figure 1. XRD pattern of the Mn_3O_4nanoparticles.

The observed peaks match the values for orthorhombic Mn_3O_4(PCPDF card no.750765). The calculated lattice parameters are a=3.06, b=9.769, c=9.568 .The particle size of the product estimated from the X-ray peak broadening of the (100) diffraction peak using the Debye Scherer formulais 50±5 nm showing that the synthesized powder contains nanometer sized crystallites.

Optical Analysis: UV-visible absorption spectra of Mn_3O_4 nanoparticle is shown in figure 2. The figure 2 shows that the absorption peaks were observed at 202 nm. From UV analysis, it came to the conclusion that the band gap of a material increases when particle size of nanoparticle decreases.

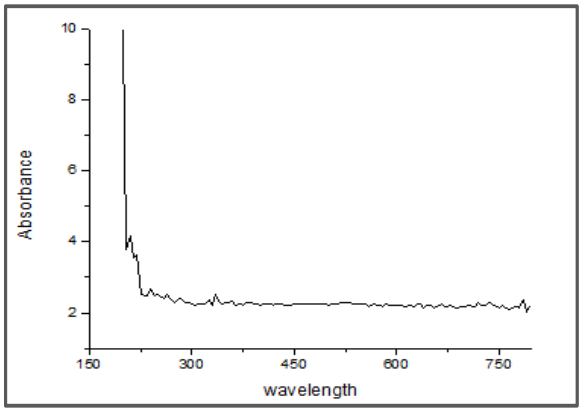

Figure 2. UV-vis absorbation spectra of Mn_3O_4 nanoparticles.

Morphological analysis: Figure 3(a,b,c) shows the SEM images of the as-prepared Mn_3O_4 nano structures by the hydrothermal process. The SEM image of Mn_3O_4 show a partial aggregation of particle with irregular shape. This aggregation of nanoparticles is due to the effect of temperature because it forms the hot surface on primarily formed nanoparticles. When increasing the reaction time above 10 min, the agglomeration of the particle gets reduced and the individual spherical like particle can be visualized. From the SEM images, it is clear that the aggregation of particles decreases and smaller nanoparticles are dissolved with increase in the reaction time, finally the individual nanospheres is formed. It infers that the reaction time does not possess the considerable morphological variations in the samples but the agglomeration of the nanoparticles gets decreased at longer reaction time. From the SEM images as shown in figure 3(a) the large quantity of sphere like

nanostructures with about 50-100 nm have been observed and the large scale Mn_3O_4 nanospheres can be confirmed by the SEM images in figure 3(c). Figure 4 shows the TEM images of the samples prepared by the subsequent annealing treatment of the as-synthesized cubic structured Mn_3O_4 nanoparticles at 300°C. From the TEM images the cubic structured nanoparticles have been obtained with the diameter of about 50-100 nm.

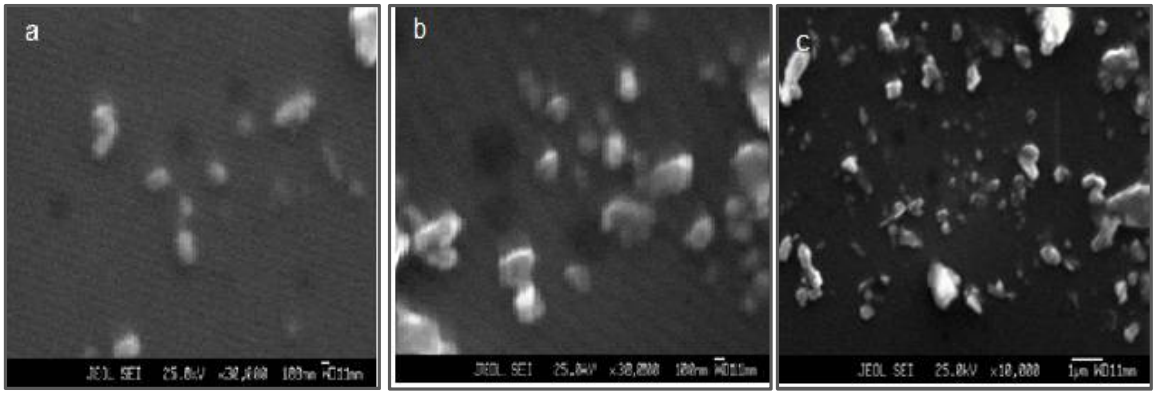

Figure 3. SEM images (a,b,c).

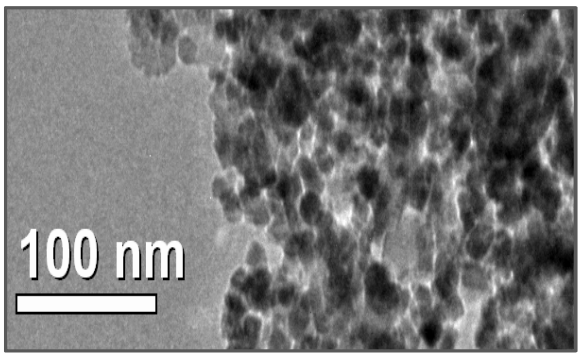

Figure 4. TEM images of the prepared Mn_3O_4 nanoparticles.

APPLICATION

The synthesized catalysts were used for the synthesis of biologically potent tetrahydro-1H-pyrano [2,3-d]pyrimidine derivatives. Pyranopyrimidine heterocyclics showed prominent biological activities and are considered required drugs in day to day life. Thus, synthesis of nanoparticle then its application on useful heterocyclic compounds emerged as an astounding reaction condition for an innovative research.

CONCLUSION

Mn_3O_4 nanoparticles were synthesized by using hydrothermal technique. The X-ray diffraction (XRD), scanning electron microscopy (SEM), was used to characterize the structure and morphology of the Mn_3O_4 nanoparticles. X-ray diffraction analysis reveals that the crystallite size of the Mn_3O_4 nanoparticles was found to be 50±5 nm. The morphology of the Mn_3O_4 nanoparticles was characterized by scanning electron microscopy. The optical properties were studied by the UV-Visible absorption spectrum. It is found that the low temperature preparation of these single crystalline nanospheres avoids the use of high violent manganese compounds or poisonous organic compounds. Moreover, this low temperature synthetic route might be a general one for the growth of single crystal of one dimensional structures of other compounds. The synthesized catalysts were used for the synthesis of biologically potent tetrahydro-1H-pyrano[2,3-d]pyrimidine derivatives. Pyranopyrimid-

ine heterocyclics showed promenet biological activities and are considered required drugs in day to day life. Thus, synthesis of nanoparticle then its application on useful heterocyclic compounds emerged as an astounding reaction condition for an innovative research.

ACKNOWLEDGEMENTS

S ShabirBhatsincerely thankDepartment of Physics National Institute of Technology Srinagar for providing XRD technique. The authorsacknowledge the National Centre of Experimental Mineralogy and Petrology University of Allahabad, India to perform SEM analysis. The authors also thanks to Sophisticated Analytical Instrument Facilities Department of Science and Technology AIIMS New Delhi to perform TEM analysis. The authors gratefully acknowledged Prof. S.K Saivastaw, Head Department of Chemistry University of Allahabad to provide the synthesis laboratory facility and also one of the author (S ShabirBhat) gratefully acknowledge Dr. Malik A Waseem Department of Chemistry University of Kashmir for his generous support during this work.

REFERENCES

[1]. Xiong Zhang, Peng Yu, Dacheng Zhang, Haitao Zhang, Xianzhong Sun, Yanwei Ma, Room temperature synthesis of Mn_3O_4 nanoparticles: characterization, electrochemical properties and hydrothermal transformation to γ-MnO_2 nanorods, *Materials Letters*, **2013**, 92, 401–404

[2]. S. L. Suib, Porous manganese oxide octahedral molecular sieves and octahedral layered materials, *Acc Chem Res*., **2008**, 41, 479–87.

[3]. Y. Li, H. Xie, J. Wang, L. Chen, Preparation and electrochemical performances of α-MnO_2 nanorod for supercapacitor, *Mater Lett*., **2011**, 65, 403–405.

[4]. Jin Du, Yongqian Gao, Lanlan Chai, Guifu Zou, Yue Li, Yitai Qian, Hausmannite Mn_3O_4 nanorods: synthesis, characterization and magnetic properties, Nanotechnology, **2006**, 17, 4923–4928.

[5]. Chunsheng Du , Jondo Yun, Randy K. Dumas , Xiaoyou Yuan, Kai Liu, Nigel D. Browning, Ning Pan, Three-dimensionally intercrossing Mn3O4 nanowires, *Acta Materialia*, 2008, 56, 3516–3522

[6]. Feilong Gong, Shuang Lu, Lifang Peng, Jing Zhou, Jinming Kong, Dianzeng Jia, Feng Li, Hierarchical Mn_2O_3 Microspheres In-Situ Coated with Carbon for Supercapacitors with Highly Enhanced Performances, Nanomaterials, **2017**, 7, 409; doi:10.3390/nano7120409.

[7]. Jie Gao, Michael A. Lowe, Hector D. Abruna, Spongelike Nanosized Mn_3O_4 as a High-Capacity Anode Material for Rechargeable Lithium Batteries, *Chem. Mater.,* **2011**, 23, 3223–3227

[8]. Chae-Yong Seong, Seung-Keun Park, Youngkuk Bae, Suyeon Yoo, Yuanzhe Piao, An acid-treated reduced graphene oxide/Mn_3O_4 nanorod nanocomposite as an enhanced anode material for lithium ion batteries, *RSC Adv*., **2017**, 7, 37502–37507.

[9]. Yanhong Zhao, Gang Chen, Chunshuang Yan, Chade Lv, Rui Wangaand Jingxue Sun, Stabilising Mn_3O_4 Nanosheet on Graphene via Forming 2D-2D Nanostructure for Improvement of Lithium Storage, *RSC Advances*., **2013**, 1-3.

[10]. Nan Li, Ji-Yu Wang, Zhao-Qing Liu, Yun-Ping Guo, Dong-Yao Wang, Yu-Zhi Su, Shuang Chen, One-dimensional ZnO/M_{n3O4} core/shell nanorod and nanotube arrays with high supercapacitive performance for electrochemical energy storage: *RSC Advances*, **2014**, 01, 000588.

[11]. Kalimuthu Vijaya Sankar, D. Kalpanaand Ramakrishnan Kalai Selvan, Electrochemical properties of microwave-assisted reflux-synthesized Mn3O4 nanoparticles in different electrolytes for supercapacitor applications, *J Appl Electrochem*., **2012**, 42, 463–470.

[12]. Zhenjun Qi, Adnan Younis, Dewei Chu, Sean Li, A Facile and Template-Free One Pot Synthesis of Mn3O4 Nanostructures as Electrochemical Supercapacitors, *Nano-Micro Letters*, **2016**, 8(2), 165-173.

[13]. Huang Tang, Yongxing Sui , Xiaoqin Zhu, Zhihao Bao, Synthesis of Mn_3O_4-Based Aerogels and Their Lithium-Storage Abilities, *Nanoscale Research Letters*, **2015**, 10, 260.
[14]. Abdulhadi Baykal, Yuksel K oseo˘glu, Mehmet, Senel, Low temperature synthesis and characterization of Mn_3O_4 nanoparticles. *CEJC*, **2007**, 5(1), 169–176
[15]. J. Li, Y. J. Wang, B. S. Zou, X. C. Wu, J. G. Lin, L. Guo, Q.S. Li, Magnetic Properties of Nanostructured Mn Oxide Particles, *Appl. Phys. Lett.*, **1997**, 70,3047–3049.
[16]. A. R. Armstrong, P. G. Bruce, Synthesis of Layered $LiMnO_2$ as an Electrode for Rechargeable Lithium Batteries, *Nature*, **1966**, 381, 499–500.
[17]. Y. F. Shen, R. P. Zerger, R. N. Deguzman, S. I. Suib, L. Mccurb, D. I. Potter, L.,L. Oyoung, Manganese Oxide Octahedral Molecular Sieves: Preparation, Characterization, and Applications, Science, **1993**, 260, 511–515.
[18]. M. C. Bernerd, H. L. Goff, B. V. Thi, Electrochromic Reactions in Manganese Oxides, *J. Electrochem. Soc*., **1993**, 140, 3065–3070.
[19]. S. H. Kim, S. J. Kim, S. M. Oh, Preparation of Layered MnO_2 via Thermal Decomposition of $KMnO_4$ and Its Electrochemical Characterizations, *Chem. Mater.*, **1999**, 11, 557–563.
[20]. W. P. Tang, H. Kanoh, X. J. Yang, K. Ooi, Preparation of Plate-Form Manganese Oxide by Selective Lithium Extraction from Monoclinic Li_2MnO_3 under Hydrothermal Conditions, Chem. Mater., **2000**, 12, 3271–3279.
[21]. Y. J. Lee, C. P. Grey, Determining the Lithium Local Environments in the Lithium Manganates LiZn0.5Mn1.5O4 and Li2MnO3 by Analysis of the 6Li MAS NMR Spinning Sideband Manifolds, *J. Phys. Chem.*, **2002**, B106, 3576–3582.
[22]. G. H. Lee, S. H. Huh, J .W. Jeong, B. J. Choi, S. H. Kim, H. C. Ri, Anomalous Magnetic Properties of MnO Nanoclusters, *J. Am. Chem. Soc*., **2002**, 124, 12094–12095.
[23]. A. H. De Vries, L. Hozoi, R. Broer, Importance of Interatomic Hole Screening in Core-level Spectroscopy of Transition Metal Oxides: Mn_3S Hole States in MnO, *Phys. Rev.,* **2002**, B 66, 35108,1-35108,10.
[24]. Y. Yamashita, K. Mukai, J. Yoshinobu, M. Lippmaa, T. Kinoshitaand M. Kawasaki, Chemical Nature of Nanostructures of $LaO_6SrO_4MnO_3$ on $SrTiO_3$(100, *Surf. Sci.*, **2002**, 514, 54–59.
[25]. Y. Chang, X. Y. Xu, X. H. Luo, C. P. Chen, D. P. Yu, Synthesis and Characterization of Mn_3O_4 Nanoparticles, *J. Cryst. Growth*, **2004**, 264, 232-236.
[26]. A. S. Fritsch, J. Sarrias, A. Rousset, G. U. Kulkarni, Low-temperature Oxidation of Mn_3O_4 Hausmannite, *Mat. Res. Bull.*, **1998**, 33(8), 1185–1194.
[27]. Y. C. Zhang, T. Qiao, X. Y. Hu, Preparation of Mn_3O_4 Nanocrystallites by Low-temperature Solvothermal Treatment of γ-MnOOH Nanowires", *J. Solid State Chem*., **2004**, 177, 4093-4097.
[28]. E. Finocchio, G. Busca, Characterization and Hydrocarbon Oxidation Activity of Coprecipitated Mixed Oxides Mn_3O_4/Al_2O_3, *Catal. Today*, **200**1, 70, 213–225.
[29]. S. K. Apte, S. D. Naik, R. S. Sonawane, B. B. Kale, N. Pavaskar, A. B. Mandale, B. K. Das, Nanosize Mn_3O_4 (Hausmannite) by a Microwave Irradiation Method, *Mater. Res. Bull*., **2006**, 41, 647–654.
[30]. A. K. M. Atique Ullah, A. K. M. Fazle Kibria, M. Akter, M. N. I. Khan, M. A. Maksud, RumanaA. Jahan, Shakhawat H. Firoz, Synthesis of Mn_3O_4 nanoparticles viaa facile gel formation route and study of its phase and structural transformation with distinct surface morphology upon heat treatment, (**2017**) JSCS 867.
[31]. J. Kaczmarek, E. Wolska, Cation and Vacancy Distribution in Nonstoichiometric Hausmanite, *J. Solid State Chem.*, 1993, 103,387-393.
[32]. J. D. Dunitz, L. E. Orgel, Electronic properties of transition-metal oxides-II, Cation distribution amongst octahedral and tetrahedral sites, *J. Phys. Chem. Solids*, **1957**, 3, 318-323.
[33]. Levent Kartal Yasin Kiliç, Servet Timur., Synthesis Of Nano-Manganese Oxide (Mn_2O_3) Particles By Using High Frequency-Induction System. November, **2017**,